$$R_{\beta\nu'\beta\nu}{}^{i}=\sum_{l_2l_3} G_{\beta\nu'\beta\nu}{}^{i}(l_2l_3)\Big[(-)^{j}\begin{pmatrix} J_f & 1 & l_3 \\ -M_f & k & M_f-k\end{pmatrix}\begin{pmatrix}1 & l_3 & l_2 \\ j & k-M_f & M_f-(j+k)\end{pmatrix}-(-)^{k}$$
$$\times\begin{pmatrix} J_f & 1 & l_3 \\ -M_f & j & M_f-j\end{pmatrix}\begin{pmatrix}1 & l_3 & l_2 \\ k & j-M_f & M_f-(j+k)\end{pmatrix}\Big], \quad \text{(A18)}$$

where (i,j,k) is again an even permutation of $(-1,0,1)$, and

$$G_{\beta\nu'\beta\nu}{}^{i}(l_2l_3)=-6(8\pi^5)^{1/2}\chi_{\nu'\nu}{}^{(f)*}\sum(-)^{j_{\nu'}+j_\nu+j_\beta+\frac{1}{2}+l_{\nu'}+l_\nu+l_\beta+M_f+\lambda+\lambda'+L+l'+l_3}\langle'|\beta\nu'\lambda'\rangle\langle|\beta\nu\lambda\rangle$$
$$\times i^{l_1+L_1}\hat{L}\hat{L}'\hat{L}_1\hat{l}_1{}^2\hat{l}\hat{l}'\hat{J}_f\hat{j}_\beta{}^2\hat{j}_\nu\hat{j}_{\nu'}\hat{\lambda}^2\hat{\lambda}'{}^2\hat{l}_2{}^2\hat{l}_3{}^2\begin{pmatrix}L' & L_1 & L\\ 0 & 0 & 0\end{pmatrix}\begin{pmatrix}l' & l_1 & l\\ 0 & 0 & 0\end{pmatrix}\begin{pmatrix} l_2 & L_1 & l_1\\ M_f-(j+k) & j+k-M_f & 0\end{pmatrix}\begin{Bmatrix} l_\beta & 1 & l_\beta\\ \frac{1}{2} & j_\beta & \frac{1}{2}\end{Bmatrix}$$
$$\times\begin{Bmatrix} J_f & 1 & l_3\\ j_{\nu'} & \frac{1}{2} & l_{\nu'}\\ j_\nu & \frac{1}{2} & l_\nu\end{Bmatrix}\begin{Bmatrix}1 & l_3 & l_2\\ l_\beta & l_{\nu'} & \lambda'\\ l_\beta & l_\nu & \lambda\end{Bmatrix}\begin{Bmatrix} l_1 & L_1 & l_2\\ l & L & \lambda\\ l' & L' & \lambda'\end{Bmatrix}h_{L_1}{}^{N'L'NL}(K)g_{l_1}{}^{n'l'nl}(Q)Y_{L_1}{}^{M_f-(j+k)*}(\omega_k). \quad \text{(A19)}$$

PHYSICAL REVIEW VOLUME 156, NUMBER 4 20 APRIL 1967

Projected Hartree-Fock Spectra of $2s$–$1d$-Shell Nuclei

M. R. GUNYE*
Atomic Energy Establishment Trombay, Bombay, India

AND

CHINDHU S. WARKE
Tata Institute of Fundamental Research, Colaba, Bombay, India

(Received 6 December 1966)

The Hartree-Fock calculations with a phenomenological internucleon residual interaction are carried out for the $2s$–$1d$-shell nuclei up to ^{25}Al. The low-lying excited states of these nuclei are obtained by projecting out good angular-momentum states from the deformed Hartree-Fock states. The energy spectra thus obtained are in good agreement with the experimental results. From the study of the odd-odd nuclei, it is found that the employed residual interaction correctly reproduces the ground-state spins of these nuclei. The binding energies calculated from the projected ground-state energies and a naive model are in very good agreement with the experimental binding energies.

1. INTRODUCTION

THE complexity of shell-model calculations for more than three nucleons prohibits any such calculations for many-nucleon systems. For nuclei in the $2s$–$1d$ shell, the shell-model calculations have been carried out in the case of at the most four particles outside the ^{16}O core.[1] Since the exact shell-model calculations for many-nucleon systems are prohibitive, attempts have been made to do the next best thing. Redlich[2] showed for the first time that the results of shell-model calculations can be reproduced by projecting the good angular-momentum states from an intrinsic determinantal state. These observations of Redlich in the $2s$–$1d$ shell were confirmed by Kurath and Picman,[3] who showed that for nuclei in the $1p$ shell as well, the projection method is a good approximation to the configuration-mixing calculations. This success of the projection method in obtaining shell-model wave functions implies that there is an underlying independent-particle behavior in these wave functions. The natural tool to study this independent-particle behavior is the Hartree-Fock (HF) method. The recent calculations of Bassichis, Giraud, and Ripka[4] clearly demonstrate that one can derive the energy spectra of nuclei in the $2s$–$1d$ shell by projecting out good angular-momentum states from an intrinsic (HF) state composed of the deformed single-particle orbitals.

With this success of the projection prescription, we

* Present address: Tata Institute of Fundamental Research, Colaba, Bombay, India.

[1] T. Inone, T. Sebe, H. Hagiwara, and A. Arima, Nucl. Phys. **59**, 1 (1964); T. Engeland and A. Kallio, *ibid.* **59**, 211 (1964).

[2] M. Redlich, Phys. Rev. **110**, 468 (1958).

[3] D. Kurath and L. Picman, Nucl. Phys. **10**, 313 (1959).

[4] W. H. Bassichis, B. Giraud, and G. Ripka, Phys. Rev. Letters **13**, 52 (1965).

felt it essential to study the general features of the projected nuclear spectra. This was done in an earlier paper.[5] It is clear that even the projection method becomes complicated for many-nucleon systems. It is, however, essential to carry out such calculations in view of the vast number of experimental data collected on the $2s$–$1d$-shell nuclei. The main motivation in this paper is to apply the mathematical technique developed in Ref. 5 to complicated systems and see whether one can find agreement with experimental findings. We have studied three cases each of even-even, odd-odd, and odd-A nuclei in the $2s$–$1d$ shell. The effect of band mixing in the case of two close-lying bands of ^{25}Al is also investigated in a certain approximation.

2. MATHEMATICAL FORMULATION

A. The HF Method

To start with, we note that in the shell-model wave functions, the radial dependence is fixed by a given harmonic-oscillator potential; only admixtures of various orbitals and spin configurations are considered. Similarly, in the self-consistent HF method employed here in the calculations of deformed orbitals, we have fixed the radial part of the wave functions by the harmonic-oscillator wave function; the self-consistency is imposed only on the orbital part of the wave function. The self-consistency consideration of the radial motion may be important for the nuclear binding-energy problem, but it is not crucial for calculating the low-energy excited states of nuclei. Further, in the HF variational calculation, we restrict ourselves to the axially symmetric deformation, meaning thereby that the deformed single-particle HF orbital has a good m quantum number, where m refers to the projection of the angular momentum on the symmetry axis. Thus the problem is to solve the eigenvalue equation

$$(T+\Gamma)\varphi_i=E_i\varphi_i \tag{1}$$

self-consistently, to obtain the energy E_i and the corresponding orbital φ_i given by

$$|\varphi_i\rangle=\sum_{ji} C_{m_iT_i}^{ji}|j_im_{iT_i}\rangle. \tag{2}$$

The single-particle operator T in Eq. (1) consists of the kinetic-energy term, the harmonic-oscillator potential, and a spin-orbit interaction term; the one-body HF potential Γ in Eq. (1) is given by

$$\Gamma_{\alpha\gamma}{}^{p(n)}=\sum_{\beta,\delta}(v_{\alpha\beta\gamma\delta}{}^{p(n)-p}\rho_{\delta\beta}{}^{p}+v_{\alpha\beta\gamma\delta}{}^{p(n)-n}\rho_{\delta\beta}{}^{n}), \tag{3}$$

where the superscript p (n) refers to proton (neutron), ρ is the density matrix, and v is the two-body interaction.

The restriction to axial symmetry in our calculations is not a serious matter, since in the projection method the effects of the "nonaxial" terms will be directly incorporated. This can be seen from the matrix elements of the two-body interaction appearing in the formulas of Sec. 2B.

B. Projected Energy Spectrum

The deformed intrinsic state of the system is the axially symmetric determinantal HF state $|\varphi_K\rangle$ characterized by the band quantum number K. This intrinsic state is composed of a superposition of states with good angular momenta J. The energies $E_K{}^J$ of these states are extracted from $|\varphi_K\rangle$ by angular-momentum projection:

$$E_K{}^J=\langle\varphi_K|HP_K{}^J|\varphi_K\rangle/\langle\varphi_K|P_K{}^J|\varphi_K\rangle, \tag{4}$$

where

$$\langle\varphi_K|HP_K{}^J|\varphi_K\rangle=(J+\tfrac{1}{2})\int_0^\pi \sin\theta d\theta d_{KK}{}^J(\theta)h_K(\theta), \tag{5a}$$

$$\langle\varphi_K|P_K{}^J|\varphi_K\rangle=p_K{}^J=(J+\tfrac{1}{2})\int_0^\pi \sin\theta d\theta \times d_{KK}{}^J(\theta)P_K(\theta), \tag{5b}$$

$$h_K(\theta)=\langle\varphi_K|He^{-i\theta J_y}|\varphi_K\rangle, \tag{6a}$$

$$P_K(\theta)=\langle\varphi_K|e^{-i\theta J_y}|\varphi_K\rangle, \tag{6b}$$

and H is the Hamiltonian of the system.

For completeness we quote the results of Ref. 5:

$$P_K(\theta)=D^N(a_{\alpha\beta})D^P(a_{\gamma\delta}), \tag{7}$$

$$h_K(\theta)=(T^P+V^{P-P})D^N(a_{\alpha\beta})+(T^N+V^{N-N})D^P(a_{\gamma\delta})+V^{P-N}, \tag{8}$$

where

$$T^N=\sum_{i=1}^{N}\sum_{ji\,ja}(j_im_i|T|j_am_i)\sum_{k=1}^{N}(-)^{i+k}C_{m_i}{}^{ji}C_{m_k}{}^{ja}d_{m_im_k}{}^{ja}(\theta)\cdot D_{i,k}{}^{N-1}(a_{\alpha\beta}),$$

$$V^{N-N}=\sum_{i<k}^{N}\sum_{ji\,jk}\sum_{ja\,ma\,jb\,mb}(j_im_i,\,j_km_k|v|j_am_a,,j_bm_b)\times\sum_{j<l}^{N}(-)^{i+j+k+l}C_{m_i}{}^{ji}C_{m_j}{}^{ja}d_{m_am_j}{}^{ja}(\theta)\cdot C_{m_k}{}^{jk}C_{m_l}{}^{jb}d_{m_bm_l}{}^{jb}(\theta)\cdot D_{ik,jl}{}^{N-2}(a_{\alpha\beta}),$$

[5] C. S. Warke and M. R. Gunye, Phys. Rev. **155**, 1084 (1967).

$$V^{P-N}=\sum_{i=1}^{P}\sum_{k=1}^{N}\sum_{j_ij_k}\sum_{j_am_aj_bm_b}(j_im_i,\,j_km_k|v|\,j_am_a,\,j_bm_b)$$
$$\times\sum_{j=1}^{P}\sum_{l=1}^{N}(-)^{i+j+k+l}C_{m_i}{}^{j_i}C_{m_j}{}^{j_a}d_{m_am_j}{}^{j_a}(\theta)\cdot C_{m_k}{}^{j_k}C_{m_l}{}^{j_b}d_{m_bm_l}{}^{j_b}(\theta)D_{k,l}{}^{N-1}(a_{\alpha\beta})D_{i,j}{}^{P-1}(a_{\gamma\delta}).$$

T^P and V^{P-P} in Eq. (8) are given by expressions similar to those for T^N and V^{N-N} with replacement of N by P. Other symbols appearing above are defined in Ref. 5.

The energy $E_K{}^J$ obtained this way has the variational character that it gives the upper bound to the actual energy of the state with the angular momentum J.

C. Band Mixing

If the HF energies $E_K{}^{\rm HF}$ and $E_{K'}{}^{\rm HF}$ corresponding to the bands K and K' are close, then it is quite likely that the projected energies $E_K{}^J$ and $E_{K'}{}^J$ will also be close. In this case, the projected energies must be corrected for band mixing. The wave function $\Psi_M{}^J$ for the state J will then be approximated by a linear combination of the two wave functions $\varphi_{MK}{}^J$ and $\varphi_{MK'}{}^J$:

$$\Psi_M{}^J=a\varphi_{MK}{}^J+b\varphi_{MK'}{}^J, \tag{9}$$

where

$$\varphi_{MK}{}^J=P_{MK}{}^J\varphi_K/[\langle P_{MK}{}^J\varphi_K|P_{MK}{}^J\varphi_K\rangle]^{1/2},$$

and where a similar relationship holds for $\varphi_{MK'}{}^J$. The energy E^J is then given by

$$E^J=(a^2E_K{}^J+b^2E_{K'}{}^J+2abE_{KK'}{}^J)\times(a^2+b^2+2abp_{KK'}{}^J), \tag{10}$$

where $E_K{}^J$ and $E_{K'}{}^J$ are given by Eq. (4) and

$$E_{KK'}{}^J=(J+\tfrac{1}{2})^2\int_0^\pi d\theta\sin\theta\,d_{MK}{}^J(\theta)\int_0^\pi d\theta'\sin\theta'\,d_{MK'}{}^J(\theta')\times h_{KK'}(\theta-\theta')/(p_K{}^Jp_{K'}{}^J)^{1/2}. \tag{11a}$$

$$P_{KK'}{}^J=(J+\tfrac{1}{2})^2\int_0^\pi d\theta\sin\theta\,d_{MK}{}^J(\theta)\int_0^\pi d\theta'\sin\theta'\,d_{MK'}{}^J(\theta')\times P_{KK'}(\theta-\theta')/(p_K{}^Jp_{K'}{}^J)^{1/2}, \tag{11b}$$

where $p_K{}^J$ and $p_{K'}{}^J$ are given by Eq. (5b) and

$$h_{KK'}(\theta-\theta')=\langle\varphi_K|He^{-i(\theta-\theta')J_y}|\varphi_{K'}\rangle; \tag{12a}$$

$$P_{KK'}(\theta-\theta')=\langle\varphi_K|e^{-i(\theta-\theta')J_y}|\varphi_{K'}\rangle. \tag{12b}$$

Minimizing E^J with respect to a and b in Eq. (10), one gets the corrected energy E^J as

$$E^J=\{\tfrac{1}{2}(E_K{}^J+E_{K'}{}^J)-A\pm[\tfrac{1}{4}(E_K{}^J-E_{K'}{}^J)^2+(E_{KK'}{}^J)^2+B]^{1/2}\}/c, \tag{13}$$

where

$$A=p_{KK'}{}^JE_{KK'}{}^J;$$
$$B=E_K{}^JE_{K'}{}^J(p_{KK'}{}^J)^2-(E_K{}^J+E_{K'}{}^J)p_{KK'}{}^JE_{KK'}{}^J; \tag{14}$$
$$C=1-(p_{KK'}{}^J)^2.$$

Thus one has to compute $E_{KK'}{}^J$ and $p_{KK'}{}^J$ in order to get the corrected energies of the two states with angular momentum J. We will carry out this band-mixing calculation in the case of ^{25}Al, where the $K=\frac{5}{2}$ and $K'=\frac{1}{2}$ bands lie very close.

3. APPLICATIONS

The projection method has been applied to calculate the low-lying energy levels of nine nuclei in the $2s$–$1d$ shell. The effective interaction used in the calculation is of the form

$$v(i,j)=\boldsymbol{\tau}_i\cdot\boldsymbol{\tau}_j(a+b\boldsymbol{\sigma}_i\cdot\boldsymbol{\sigma}_j)v_0e^{-r_{ij}/\mu}/(r_{ij}/\mu), \tag{15}$$

with $\mu=1.37$ F. The radial wave functions used in the calculation of matrix elements are those of harmonic oscillator with size parameter $(\hbar/M\omega)^{1/2}=1.65$ F. The calculations are done by taking $a=0.10$ and $b=0.233$ and also by taking $a=0.056$ and $b=0.233$ in Eq. (15). The results for both these sets are found to be almost the same for all the nuclei studied, and hence we have chosen to show the results obtained with Rosenfeld mixture ($a=0.10$ and $b=0.233$). In the case of ^{25}Al, however, there is some significant difference between the results obtained with two sets; therefore, we will present both results. The strength parameter v_0 in Eq. (15) is taken to be 45 MeV; the single-particle energies are fixed by the strength α of the spin-orbit force, which is taken to be -2.48 MeV. These parameters are in the same range as those employed by Kelson and Levinson.[6]

We have also carried out some calculations using the following interaction:

$$v(i,j)=\boldsymbol{\tau}_i\cdot\boldsymbol{\tau}_j(0.1+0.233\boldsymbol{\sigma}_i\cdot\boldsymbol{\sigma}_j)\times\chi\sum_M q_M(i)(-)^Mq_{-M}(j), \tag{16}$$

where $q_M=(16\pi/5)^{1/2}r^2Y_{2M}$ and χ is the strength of the quadrupole interaction.

A. Even-Even Nuclei

We have considered three nuclei, ^{20}Ne, ^{24}Mg, and ^{22}Ne, with even numbers of protons and neutrons. Figure 1(a) shows the results of calculation for ^{20}Ne with varying v_0 and keeping α fixed; the results obtained by varying α and keeping v_0 fixed are shown in Fig. 1(b). The experimental energy spectrum of ^{20}Ne is shown in Fig. 1(c). It is seen that the effect of variation of α on

[6] I. Kelson and C. Levinson, Phys. Rev. **134**, B269 (1964); J. Bar-Touv and I. Kelson, *ibid.* **138**, B1035 (1965).

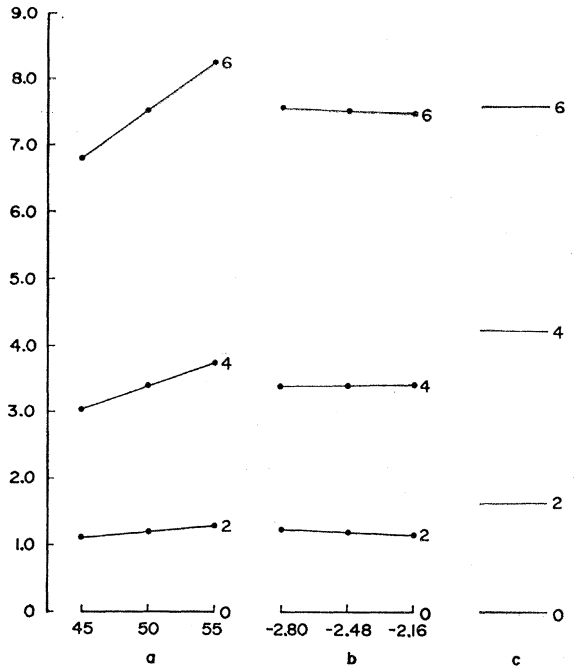

FIG. 1. Energy levels of ^{20}Ne: (a) calculated energy spectrum for $\alpha=-2.48$ MeV and v_0 varied between 45 and 55 MeV; (b) calculated energy spectrum with $v_0=50$ MeV and α varied from -2.16 to -2.80 MeV; (c) experimental spectrum. The energy scale is in MeV in this and following diagrams. The numbers on the right in each case give the spins of the levels.

the energy levels is not very significant, whereas that of variation of v_0 is quite significant; in particular, we note that the separation of higher angular-momentum

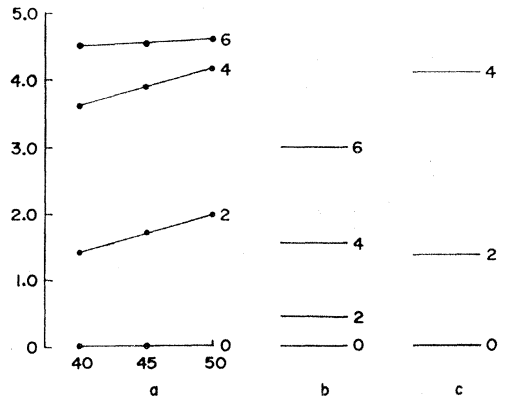

FIG. 2. Energy levels of ^{24}Mg: (a) calculated energy spectrum for $\alpha=-2.48$ MeV and v_0 varied between 40 and 50 MeV; (b) calculated energy spectrum with $v_0=45$ MeV and single-particle energy taken from ^{17}O; (c) experimental spectrum.

states from the ground state increases appreciably with increasing v_0. Similar variation is found in the case of ^{24}Mg as well. It should be mentioned that the levels do not cross; only the relative separation is affected by changing v_0 or α. The results of calculation for ^{24}Mg are shown in Fig. 2(a); the corresponding experimental energy spectrum is shown in Fig. 2(c). The calculated energy spectrum of ^{24}Mg obtained by employing the single-particle energies from ^{17}O is shown in Fig. 2(b). It is clear that the ^{17}O single-particle energy spectrum gives poor results for ^{24}Mg. The calculated and experimental energy spectra of ^{22}Ne are shown in Figs. 3(a) and 3(b), respectively.

B. The Odd-Odd Nuclei

The calculations reported in this section are done with a view to testing the reliability of the Rosenfeld mixture (with Yukawa radial dependence) in explaining the observed spins of odd-odd nuclei. If the last odd

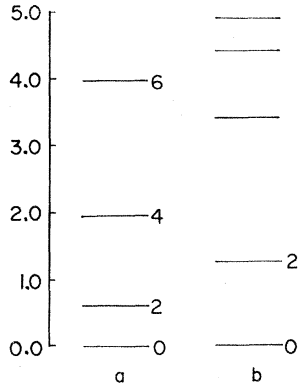

FIG. 3. Energy levels of ^{22}Ne: (a) calculated energy spectrum with $v_0=45$ MeV and $\alpha=-2.48$ MeV; (b) experimental spectrum.

proton is in the deformed HF orbital m_p and the last odd neutron is in the deformed HF orbital m_n, the two possible states of the odd-odd nucleus would correspond to the band quantum numbers $K=m_p+m_n$ and $K'=|m_p-m_n|$. The well-known rule which provides a choice between the K and K' states is due to Gallagher and Moszkowski.[7] In the case of large deformations, they predict that, of the two possibilities, the one which keeps the intrinsic spins parallel will be favored. This could arise from an $A_\sigma\boldsymbol{\sigma}_1\cdot\boldsymbol{\sigma}_2$ force with $A_\sigma<0$. It is also known[8] that an isospin-dependent term $B_\tau\boldsymbol{\tau}_1\cdot\boldsymbol{\tau}_2$ with $B_\tau>0$ can also predict the correct ground-state band of the odd-odd nuclei in $2s$-$1d$ shell. The relative importance of the spin-dependent and isospin-dependent

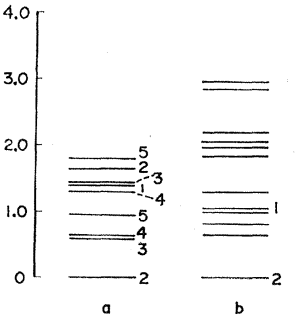

FIG. 4. Energy levels of ^{20}F: (a) calculated energy spectrum with $v_0=45$ MeV and $\alpha=-2.47$ MeV; (b) experimental spectrum.

[7] C. J. Gallagher and S. A. Moszkowski, Phys. Rev. **111**, 1282 (1958).
[8] M. R. Gunye and S. Das Gupta, Nucl. Phys. **89**, 443 (1966).

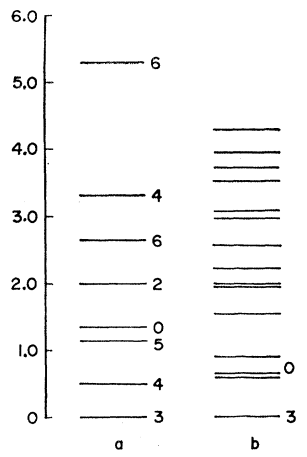

FIG. 5. Energy levels of ^{22}Na: (a) calculated energy spectrum with $v_0=45$ MeV and $\alpha=-2.48$ MeV; (b) experimental spectrum.

terms is not well known. The Rosenfeld mixture has both the spin- and isospin-dependent terms, and it was felt worthwhile to investigate whether it would reproduce the experimental result.

Generally, the HF energies $E_K{}^{\mathrm{HF}}$ and $E_{K'}{}^{\mathrm{HF}}$, corresponding to the two bands $K=m_p+m_n$ and $K'=|m_p-m_n|$ are quite close. Even though $E_K{}^{\mathrm{HF}}<E_{K'}{}^{\mathrm{HF}}$, it is not obvious that the band quantum number of the ground state is K. It would be so only if the projected energy $E_K{}^{J=K}$ is lower than the projected energy $E_{K'}{}^{J'=K'}$. The problem we want to solve is twofold: whether the employed two-body interaction

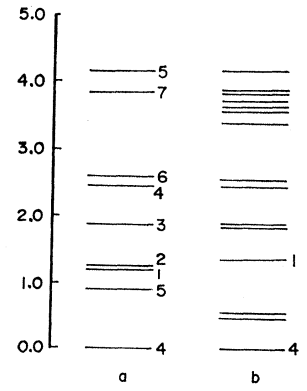

FIG. 6. Energy levels of ^{24}Na: (a) calculated energy spectrum with $v_0=45$ MeV and $\alpha=-2.48$ MeV; (b) experimental spectrum.

gives the observed spin for the ground state and also the experimental energy separation $(E_K{}^{J=K}-E_{K'}{}^{J'=K'})$ between the two states.

We have considered three odd-odd nuclei: ^{20}F, ^{22}Na, and ^{24}Na. The 9th, 11th, and 13th neutrons (or protons) go into $|m|=\frac{1}{2}, \frac{3}{2}$, and $\frac{5}{2}$ states, respectively. This gives two possibilities: $K=2$ and $K'=1$ for ^{20}F; $K=3$ and $K'=0$ for ^{22}Na; and $K=4$ and $K'=1$ for ^{24}Na. In all three cases, we find, for the same parameters: $v_0=45$ MeV and $\alpha=-2.48$ MeV, that $E_K{}^{\mathrm{HF}}<E_{K'}{}^{\mathrm{HF}}$ and also $E_K{}^{J=K}<E_{K'}{}^{J'=K'}$, in agreement with experiment. The separation $E_K{}^{J=K}-E_{K'}{}^{J'=K'}$ is also in fairly good agreement. Moreover, the slight variation in v_0 and α does not change the general trend. The projected spectra for ^{20}F, ^{22}Na, and ^{24}Na are shown in Figs. 4(a), 5(a), and 6(a), respectively; the corresponding experimental energy spectra are shown in Figs. 4(b), 5(b), and 6(b), respectively.

C. The Odd-A Nuclei

We have considered three odd-A nuclei: ^{21}Ne, ^{23}Na, and ^{25}Al. The experimental information about the first two nuclei is scarce in regard to the spins of the excited states. In the case of ^{25}Al, however, the experimental information is abundant and the spins of all the low-lying excited states are known. The calculated spectra of ^{21}Ne and ^{23}Na are shown in Figs. 7(a) and 8(a),

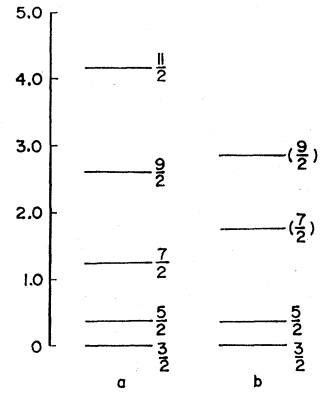

FIG. 7. Energy levels of ^{21}Ne: (a) calculated energy spectrum with $v_0=45$ MeV and $\alpha=-2.48$ MeV; (b) experimental spectrum.

respectively; the corresponding experimental results are shown in Figs. 7(b) and 8(b), respectively. The agreement between the calculated and the experimental spectra in the case of ^{21}Ne is fair; in the case of ^{23}Na, however, the agreement is poor. Experimentally, no level is yet seen between 0.438 MeV ($J=\frac{5}{2}$) and 2.08 MeV, whereas the projected $J=\frac{7}{2}$ and $J=\frac{9}{2}$ levels are at 1.06 and 1.58 MeV, respectively. On increasing the strength v_0 from 45 to 50 MeV, the projected energies come a little higher, but the experimental spectrum is not completely explained. It is possible that the observed levels at 2.08 and 2.70 MeV have spins $\frac{9}{2}$ and 11/2, and the level with spin $\frac{7}{2}$ is probably below 2.08 MeV and not yet seen.

The projected energy spectra from $K=\frac{5}{2}$ and $K'=\frac{1}{2}$ bands of ^{25}Al are shown in Fig. 9(a). Since the two bands

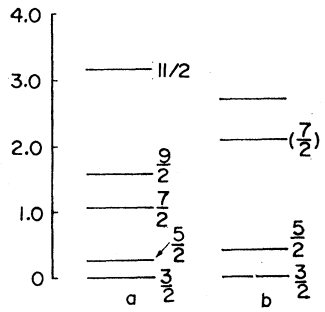

FIG. 8. Energy levels of ^{23}Na: (a) calculated energy spectrum with $v_0=45$ MeV and $\alpha=-2.48$ MeV; (b) experimental spectrum.

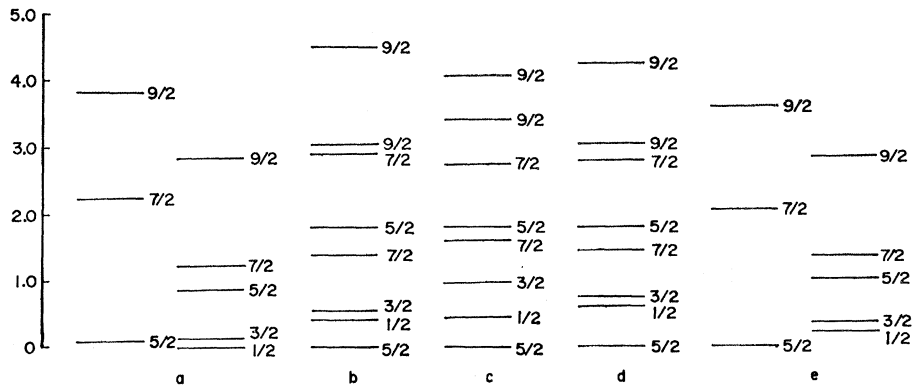

FIG. 9. Energy levels of ^{25}Al: (a) calculated energy spectrum with $v_0=45$ MeV and $\alpha=-2.48$ MeV; (b) the resultant spectrum after band mixing; (c) experimental spectrum; (d) the resultant spectrum after band mixing; (e) calculated energy spectrum with $v_0=42.5$ MeV and $\alpha=-2.48$ MeV [in this case $a=0.056$ and $b=0.233$ in Eq. (15)].

and the projected energies are quite close, the interaction between the projected states with the same angular momentum must be taken into account. The calculations for ^{25}Al are, however, very lengthy, even considering the projection from an individual band, since one has to deal with 9 particles outside the ^{16}O core. In particular, the exact band-mixing calculations described in Sec. 2C are quite involved, and hence the following approximations are sought.

The overlap integral $p_{KK'}{}^J$ in Eq. (10) is neglected. Further, the interband energy term $E_{KK'}{}^J$ in Eq. (10) is simplified by expanding the matrix element $h_{KK'}\times(\theta-\theta')$ in powers of $(\theta-\theta')$ and neglecting the terms of powers greater than 4:

$$h_{KK'}(\theta-\theta')=\langle\varphi_K|He^{-i(\theta-\theta')J_y}|\varphi_{K'}\rangle$$
$$=\sum_{n=1}^{\infty}\frac{(-)^n}{(2n)!}(\theta-\theta')^{2n}\langle\varphi_K|HJ_y{}^{2n}|\varphi_{K'}\rangle, \quad (17)$$

since K and K' differ by 2 in the case of the two bands of ^{25}Al under consideration, and consequently

$$\langle\varphi_K|HJ_y{}^n|\varphi_{K'}\rangle=0 \quad \text{for odd } n,$$
$$\langle\varphi_K|H|\varphi_{K'}\rangle=0.$$

It is verified that the most important term in Eq. (17) is that with $n=1$; the $n=2$ term is also quite substantial, but the higher terms can be neglected, as their contribution is small. Hence we have

$$h_{KK'}(\theta-\theta')\approx-\tfrac{1}{2}(\theta-\theta')^2\langle\varphi_K|HJ_y{}^2|\varphi_{K'}\rangle$$
$$+(1/24)(\theta-\theta')^4\langle\varphi_K|HJ_y{}^4|\varphi_{K'}\rangle.$$

This simplifies Eq. (11) to the form

$$E_{KK'}{}^J=(J+\tfrac{1}{2})^2[\lambda_1 f_2(J)+\lambda_4 F_4(J)]/(p_K{}^J p_{K'}{}^J)^{1/2},$$

where

$$f_2(J)=-\frac{1}{2}\int_0^\pi \sin\theta d\theta d_{MK}{}^J(\theta)\int_0^\pi \sin\theta' d\theta'$$
$$\times(\theta-\theta')^2 d_{MK'}{}^J(\theta'),$$
$$f_4(J)=\frac{1}{24}\int_0^\pi \sin\theta d\theta d_{MK}{}^J(\theta)\int_0^\pi \sin\theta' d\theta'$$
$$\times(\theta-\theta')^4 d_{MK'}{}^J(\theta').$$

Since $E_{KK'}{}^J$ is independent of M, we have chosen a value of M for which $f_2(J)/f_4(J)$ is fairly constant for $J=\frac{5}{2},\frac{7}{2}$ states, and then we can write

$$E_{KK'}{}^J=(J+\tfrac{1}{2})^2\lambda f_2(J)/(p_K{}^J p_{K'}{}^J)^{1/2}. \quad (18)$$

We fixed λ from the two $\frac{5}{2}$ states in ^{25}Al and then calculated the energies of other states by using this value of λ. The resultant spectrum after taking into account the band mixing between the $K=\frac{5}{2}$ and $K'=\frac{1}{2}$ bands is shown in Fig. 9(b). The experimental spectrum is shown in Fig. 9(c). The agreement between the calculated and the experimental spectrum is fair in the sense that the trend is correctly reproduced. For detailed agreement, it is essential to carry out the exact band-mixing calculations. We have also shown the energy spectra calculated by employing $a=0.056$ and $b=0.233$ in Eq. (15) for comparison. Fig. 9(e) shows the spectra projected from $K=\frac{5}{2}$ and $K'=\frac{1}{2}$ bands; the spectrum obtained by taking band mixing into account is shown in Fig. 9(d).

D. Calculations with the Quadrupole Force

We have used the modified quadrupole interaction in Eq. (16) to calculate the projected HF spectra of ^{19}F, ^{20}F, and ^{20}Ne. The single-particle energies are taken from ^{17}O spectrum; the strength χ was varied. The results for $\chi=0.10$ (in units of $M^2\omega^4$/MeV) are shown. Figures 10(a), 10(c), and 10(e) show the projected spectra of ^{20}Ne, ^{19}F, and ^{20}F, respectively; the corresponding experimental results are shown in Figs. 10(b), 10(d), and 10(f), respectively. A qualitative agreement certainly exists. However, the states with higher angular momentum come too high, showing thereby that this interaction is inferior to that used earlier.

E. Binding Energies

In calculating the binding energies B of the $2s$–$1d$-shell nuclei, we assume that the core (i.e., ^{16}O) is inert. The binding energy of the outer nucleons is equal to the projected ground-state energy E_G plus the contribution from the external nucleon-core interaction. In order to calculate the latter, we assume that the

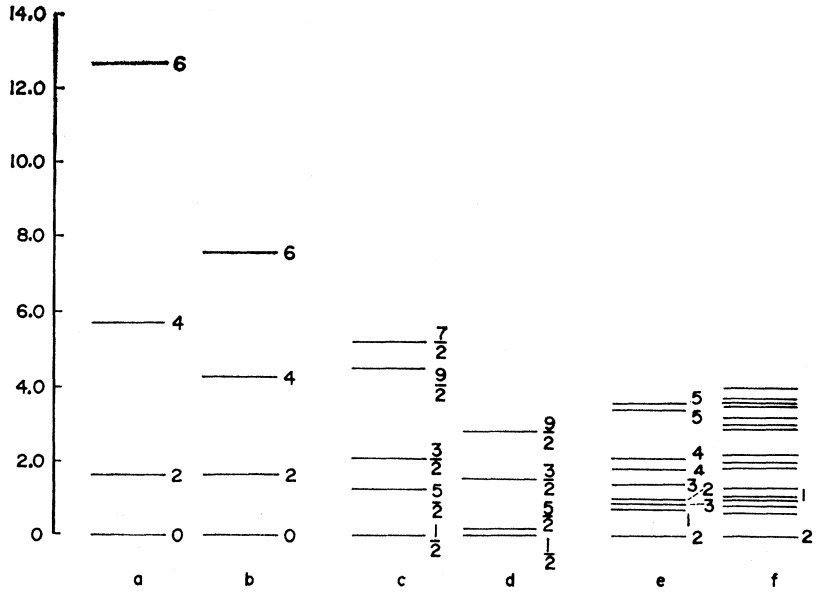

FIG. 10. Results of calculations with residual interaction in Eq. (16) with $\chi=0.10$ (in units of $M^2\omega^4$/MeV). The single-particle energies are taken from the ^{17}O spectrum. (a) The calculated energy spectrum of ^{20}Ne. (b) Experimental spectrum of ^{20}Ne. (c) Calculated spectrum of ^{19}F. (d) Experimental spectrum of ^{19}F. (e) Calculated spectrum of ^{20}F. (f) Experimental spectrum of ^{20}F.

nucleon-core contribution to the binding energy is constant λ per particle. With this, we have for the B of a nucleus (^{16}O+n), where n is the number of outer nucleons:

$$B(^{16}\mathrm{O}+n)=B(^{16}\mathrm{O})-E_G(n)+\lambda n. \qquad (19)$$

We fix λ by fitting the B of ^{20}F. With this value of λ, the calculated results are shown in Table I. The agreement is much better than expected.

TABLE I. The experimental binding energy B is given in the second column. The calculated B with (i) $v_0=45$ MeV, $a=0.10$, $b=0.233$ and (ii) $v_0=42.5$ MeV, $a=0.056$, $b=0.233$ in Eq. (15) are shown in the third and fourth columns, respectively. The B of the ^{16}O core is excluded in the tabulated values. The projected ground-state energies (E_G) corresponding to the cases (i) and (ii) are shown in the fifth and sixth columns, respectively.

Nucleus	Experimental B (MeV)	Calculated B (i) (MeV)	Calculated B (ii) (MeV)	E_G (i) (MeV)	E_G (ii) (MeV)
^{20}F	26.78	26.78	26.78	19.37	18.14
^{20}Ne	33.27	36.40	35.02	28.99	26.38
^{21}Ne	40.02	41.79	40.56	32.53	29.76
^{22}Ne	50.39	48.98	48.02	37.87	35.06
^{22}Na	46.77	50.33	48.65	39.22	35.69
^{23}Na	59.18	58.88	57.19	45.92	42.07
^{24}Na	66.14	65.74	64.23	50.93	46.95
^{24}Mg	70.88	72.12	69.47	57.31	52.19
^{25}Al	73.18	79.71	77.09	63.05	57.65

4. CONCLUSIONS

It is found that the phenomenological nucleon-nucleon potential such as the Rosenfeld mixture with Yukawa radial dependence explains the low-lying energy levels of nuclei in the $2s$–$1d$ shell fairly well. For the fixed strength v_0 of the internucleon potential and the fixed single-particle energy spectrum, the calculated low-lying excited states of the nuclei considered in this paper are in good agreement with the experimental results. The single-particle energies as taken from the ^{17}O spectrum do not give good results for a large number of nucleons outside the ^{16}O core. For detailed agreement between the calculated and the experimental results, the nucleon-number (A) dependence of v_0 and the single-particle energies is needed. No attempt is made to investigate it. The binding energies of the nuclei calculated with the crude model are in very good agreement with the experimental binding energies. The quadrupole force, though it qualitatively explains the low-lying excited states, has the bad feature that the large-angular-momentum states lie very much higher than the experimental results. From the study of odd-odd nuclei, it is found that the Rosenfeld mixture has the correct character to reproduce their ground-state spins. In general, it is clear from these calculations that the projected HF spectra do resemble closely the experimental energy spectra.